J. Fluid Mech. (1978), *vol.* 86, *part* 1, *pp.* 33–47
Printed in Great Britain

Theory of vortex nutation and amplitude oscillation in an inviscid shear instability

By AKIRA MIURA AND TETSUYA SATO

Geophysics Research Laboratory, University of Tokyo, Japan

(Received 19 November 1976 and in revised form 12 July 1977)

In the first part of this paper the nonlinear development of the most unstable mode is numerically studied for a bounded shear layer with a hyperbolic-tangent profile. It is found that the vortex nutation, discovered by Zabusky & Deem (1971) for a jet profile, is a manifestation of strongly coupled oscillations in the vortex amplitude and the phase. In the second part, with the aid of the numerical result we devote ourselves to deriving coupled nonlinear equations that describe the amplitude oscillation, the vortex nutation and the momentum transport. The approximate oscillatory solution for the vortex amplitude and phase in the nonlinear stage is compared with the numerical solution and agreement is found.

1. Introduction

It is well known that a velocity shear has a great influence upon the stability of hydrodynamic flows and plasma flows. In recent years extensive numerical calculations have been carried out to investigate the nonlinear evolution of two-dimensional shear instabilities (see, for example, Levy & Hockney 1968; Zabusky & Deem 1971; Christiansen & Zabusky 1973; Tanaka 1975). These calculations have shown that unstable modes undergo quasi-periodic amplitude oscillations in the nonlinear stage.

The nonlinear development of an electrostatic shear instability in a magnetized plasma was investigated numerically by Byers (1966) for a low density magnetized plasma where $\omega_{pi}^2 \ll \Omega_i^2$ (ω_{pi} is the ion plasma frequency and Ω_i is the ion Larmor frequency) and by Levy & Hockney (1968) for a low density magnetized electron beam. These numerical calculations have succeeded in demonstrating the formation of vortices. In particular, Levy & Hockney have recognized in their numerical experiment that there is a quasi-periodic exchange of energy between the mean flow and the most unstable mode.

The hydrodynamic shear instability has a much longer history. Sato & Kuriki's (1961) wake experiment may be a notable classical experiment. Zabusky & Deem (1971) attempted to analyse synergetically the nonlinear evolution of an unstable two-dimensional staggered-vortex wake. They found that even in the nonlinear stage the disturbance amplitude does not reach a steady state, but instead exhibits a low frequency nonlinear oscillation in conjunction with a nearly periodic phase reversal. They noticed that this amplitude oscillation is associated with a 'nutation' of the principal axis of an elliptical vortex with respect to the mean flow and that the nutation frequency is only weakly dependent on viscosity. In addition, by examining the evolution of each Fourier component of the disturbance they concluded that the interaction between the mean flow and the most unstable mode of the disturbance is responsible for the observed amplitude oscillation. Furthermore, Christiansen & Zabusky (1973) have examined in detail the stability and long-time evolution of two-dimensional wakes. Since several fundamental characteristics inherent in the two-dimensional wake such as the vortex nutation and the enhanced transport associated with the unstable disturbance are elucidated in this work, readers should consult this work. It should also be noted that a simpler example of vortex nutation was discussed by Moore & Saffman (1971).

From the analytical side, much effort has so far been devoted to the study of instabilities of parallel shear flows. Meksyn & Stuart (1951) solved a set of linearized equations for the most unstable mode and the mean motion to find an equilibrium solution for viscous fluids. Later, Stuart (1958) extended a nonlinear theory of parallel shear flows by introducing the so-called shape assumption: that a disturbance keeps its initial shape during the course of nonlinear evolution. Since these authors were primarily interested in the equilibrium state which would be realized by the balance between the linear growth and the viscous dissipation, they did not notice the existence of a phase difference between the mean motion and the vortex motion. For an inviscid fluid, Schade (1964) calculated the equilibrium amplitude of a neutral disturbance. Recently, on the basis of the shape assumption, Tanaka (1975) has calculated the maximum amplitude of the most unstable mode by numerically integrating the amplitude equation.

As we have seen above, considerable progress has been achieved in the understanding of the nonlinear behaviour of a shear instability. Notwithstanding, the fundamental processes in the nonlinear stage, i.e. the quasi-periodic oscillations in the amplitude and the associated quasi-periodic phase inversions observed by Levy & Hockney (1968), Zabusky & Deem (1971), Christiansen & Zabusky (1973) and Tanaka (1975), are still unresolved theoretically. The principal aim of this paper is to elucidate the fundamental process of the periodicity.

In the conventional analysis based on the shape assumption (e.g. Stuart 1958; Tanaka 1975) attention was paid only to the time evolution of the amplitude function, and the time evolution of the phase function was completely disregarded. Because of this one-sided choice they were not able to explain the amplitude oscillation phenomena observed. Since the inclination of the vortex axis is mainly determined by the phase of the complex stream function, it is absolutely essential to take into account the temporal variation of the phase function as well as the amplitude function if one wishes to elucidate the amplitude oscillation or the vortex 'nutation'.

It is to be noted that an extension of Landau–Stuart theory which expands the amplitude as the only small parameter cannot obtain the vortex nutation no matter how higher-order corrections are renormalized as was done by Michalke (1965).

In § 2 the amplitude and phase evolution of the most unstable disturbance are numerically examined for a bounded shear layer (i.e. a 'tanh' profile with boundary conditions at a finite distance) and a one-to-one correspondence between the evolution of the amplitude and that of the phase is verified. In the course of this numerical analysis it is found that the mean flow undergoes the same periodic modulation. In § 3 we devote ourselves to developing a theory that can elucidate the fundamental nonlinear process producing the vortex nutation.

2. Numerical results

Let us consider a two-dimensional inviscid fluid flow in the x, y plane. The equation for the vorticity $\zeta(x, y, t)$ is written as

$$\frac{\partial \zeta}{\partial t}+u\frac{\partial \zeta}{\partial x}+v\frac{\partial \zeta}{\partial y} = 0, \tag{2.1}$$

with

$$u = \frac{\partial \psi}{\partial y}, \quad v = -\frac{\partial \psi}{\partial x}, \quad \zeta = \frac{\partial v}{\partial x}-\frac{\partial u}{\partial y} = -\nabla^2 \psi, \tag{2.2a–c}$$

where ψ is the stream function.

We assume that the undisturbed flow velocity $\mathbf{V}$ has only a y component and is sheared in the x direction, i.e. $\mathbf{V} = (0, V(x), 0)$. As the profile of $V(x)$ we adopt a hyperbolic-tangent velocity profile ('tanh' profile) such that

$$\mathbf{V}(x) = V(x)\,\hat{\mathbf{y}} = V_0 \tanh(x/a)\,\hat{\mathbf{y}}, \tag{2.3}$$

where $\hat{\mathbf{y}}$ is a unit vector along the y axis and $V_0 > 0$.

Now we put

$$\psi(x,y,t) = \Psi(x)+\phi(x,y,t), \tag{2.4}$$

where $\Psi(x)$ and $\phi(x,y,t)$ are the undisturbed and disturbed parts of the stream function, respectively, and expand the disturbed part $\phi(x,y,t)$ in a Fourier series with respect to y, namely

$$\phi(x,y,t) = \sum_p \phi_p(x,t)\exp(ipky), \tag{2.5}$$

where k is the wavenumber of the most unstable mode and the summation extends over $p = 0, \pm 1, \pm 2, \ldots$. The reality of ϕ gives

$$\phi_p^* = \phi_{-p}, \tag{2.6}$$

where the asterisk denotes the complex conjugate.

The mean part of the stream function, $\bar{\psi}(x,t)$, and that of the longitudinal velocity component, $\bar{v}(x,t)$, are expressed as

$$\bar{\psi}(x,t) = \Psi(x)+\phi_0(x,t), \quad \bar{v}(x,t) = V(x)-\partial\phi_0/\partial x. \tag{2.7}$$

Since we are primarily interested in the amplitude oscillation that may result from a periodic energy exchange between the mean flow and the fundamental mode, we shall disregard higher harmonics and retain only terms with $p = 0, \pm 1$ in (2.5). Substitution of (2.5) with $p = 0, \pm 1$ into (2.1) and (2.2) yields a set of equations for each Fourier component which is solvable by a finite-difference method (see appendix). In the actual calculation, we have chosen the following normalization units of time (t_0), length (L) and stream function (Ψ_0):

$$t_0 = \gamma_{\text{lin}}^{-1}, \quad L = 2a, \quad \Psi_0 = LV_0 = 2aV_0, \tag{2.8}$$

where γ_{lin} denotes the linear growth rate for the most unstable mode. The values of γ_{lin} and k are determined by numerically integrating the Rayleigh stability equation for an unbounded tanh velocity profile (Michalke 1964):

$$\gamma_{\text{lin}} = 0{\cdot}1897\,V_0/a, \quad k = 1/2{\cdot}249a. \tag{2.9}$$

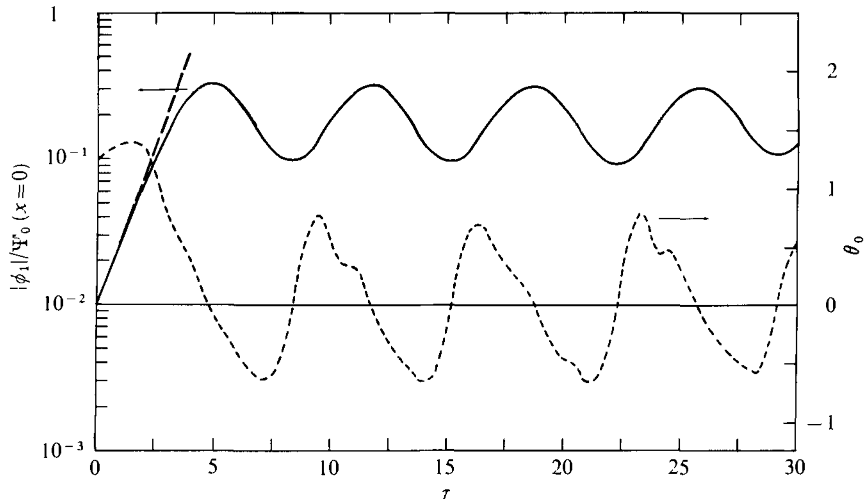

FIGURE 1. Temporal evolution of the disturbance amplitude $|\phi_1|$ at $x = 0$ (solid curve) and the phase inclination factor θ_0 defined in (2.14) (dashed curve). The temporal evolution of $|\phi_1|$ expected from the linear theory is shown by the dashed straight line.

In our calculation, a bounded layer with boundary conditions at a finite distance is assumed. Namely, we put two plane boundaries on which

$$\phi = 0 \tag{2.10}$$

at $x = \pm b$, where b is chosen to be

$$b = 2L. \tag{2.11}$$

The following initial disturbance is chosen:

$$\left.\begin{aligned} \phi_0(x, 0) &= 0, \\ \mathrm{Re}\,[\phi_1(x, 0)] &= 0{\cdot}01\Psi_0 \cos(\pi x/2b) \cos[\tfrac{1}{2}\pi \sin(\pi x/2b)], \\ \mathrm{Im}\,[\phi_1(x, 0)] &= 0{\cdot}01\Psi_0 \cos(\pi x/2b) \sin[\tfrac{1}{2}\pi \sin(\pi x/2b)], \end{aligned}\right\} \tag{2.12}$$

where Re and Im denote the real and imaginary parts, respectively.

In order to facilitate comparison with the theoretical result in § 3, we shall express the output of $\phi_1(x, t)$ in terms of its absolute value and a phase angle defined by

$$\Theta_1(x, t) = \arctan(\mathrm{Im}\,\phi_1/\mathrm{Re}\,\phi_1). \tag{2.13}$$

In practice, it may be more convenient to use, in place of $\Theta_1(x, t)$, a phase inclination factor θ_0 defined by

$$\theta_0 = L[\partial\Theta_1/\partial x]_{x=0}. \tag{2.14}$$

The solid curve in figure 1 shows the time evolution of the amplitude $|\phi_1|$ of the stream function normalized by Ψ_0 at the centre of the shear layer, while the dashed curve shows the evolution of the phase inclination factor θ_0 defined above. Until about $\tau = 1{\cdot}0$ ($\tau = t/t_0$) the amplitude is seen to continue to grow with a constant exponential slope from its initial value. For comparison, the time evolution expected from the linear theory is shown as a dashed straight line. The observed amplitude at $x = 0$ becomes at $\tau = 1{\cdot}0$

$$|\phi_1/\Psi_0| = 2{\cdot}730 \times 10^{-2}, \tag{2.15}$$

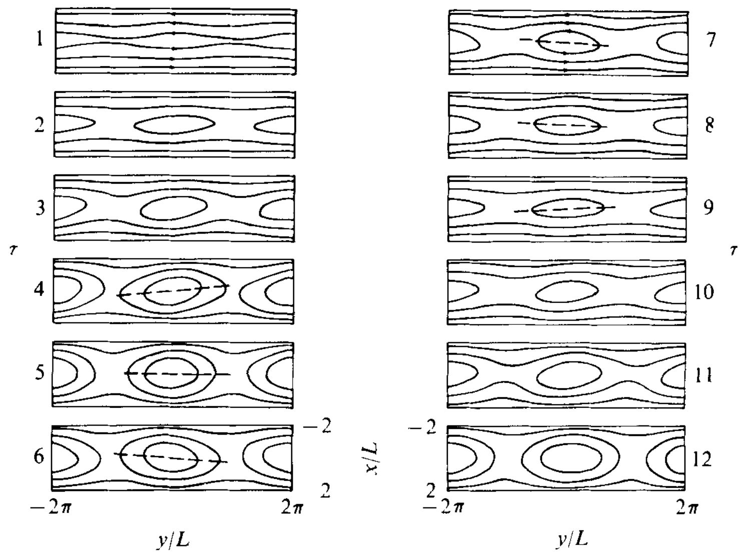

FIGURE 2. Temporal variation of the patterns of the streamlines. Arrows indicate the flow direction.

so that the observed growth rate is in good agreement with γ_{11n}. This good agreement between the linear theory and the numerical calculation ensures that the initial disturbance (2.12) adopted gives a good approximation to the exact eigenfunction of the Rayleigh stability equation for the unbounded case. From this figure it is seen that the amplitude reaches its first maximum at about $\tau = 4{\cdot}875$, when

$$|\phi_1/\Psi_0| = 3{\cdot}32\times 10^{-1}. \tag{2.16}$$

After attaining the first maximum, it begins to decrease and then grows, thereafter repeating a periodic excursion, i.e. it oscillates. The ensuing maximum amplitudes are found to be almost the same as the first one, given by (2.16). The first minimum appears at about $\tau = 8{\cdot}375$ and its value is

$$|\phi_1/\Psi_0| = 9{\cdot}63\times 10^{-2}, \tag{2.17}$$

which roughly holds for the ensuing minima. The period T_0 of the amplitude oscillation is about

$$T_0 \approx 7{\cdot}0t_0. \tag{2.18}$$

Let us turn our attention to the time evolution of the phase inclination factor θ_0. It is evident in the figure that θ_0 oscillates in accord with the amplitude oscillation. In particular, θ_0 is positive while the amplitude is growing but negative while it is decaying and tends to be zero whenever the amplitude approaches an extremum. These results strongly indicate that temporal variation of the phase function of the disturbance plays a crucial role in the amplitude oscillation process.

The streamline patterns at different times are illustrated in figure 2. As can be seen from the top left panel of the figure, which corresponds to $\tau = 1{\cdot}0$, the streamlines still remain rather straight. For the panels corresponding to times after $\tau = 2{\cdot}0$, however, we can recognize the appearance of clear-cut vortices. This figure does indicate that the vortices exhibit a periodic nutation; that is to say, the inclination of

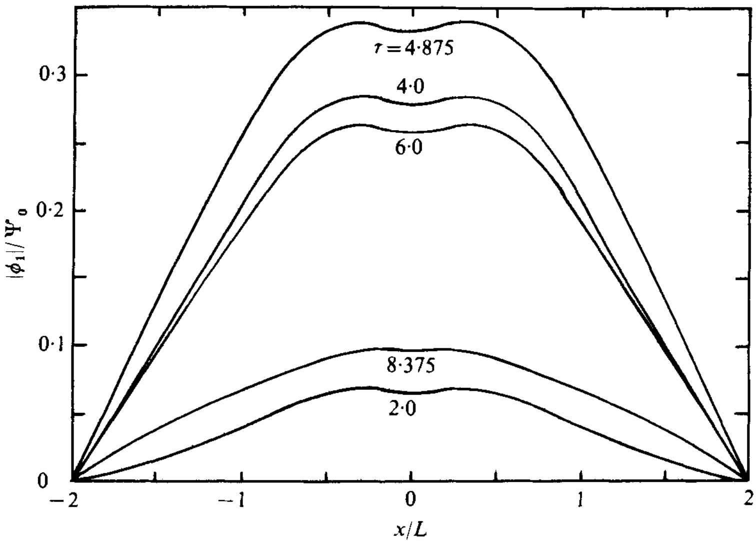

FIGURE 3. Amplitude functions $|\phi_1|$ of the disturbance at several different times.

the major axes of the elliptical vortices with respect to the mean flow direction changes in a periodic manner. Detailed comparison between this and the time evolution of the amplitude shown in figure 1 makes it clear that the major axis of a vortex is inclined against the mean flow direction while the amplitude is growing but inclined towards the mean flow direction during the amplitude's decaying phase. Because of this similarity, it may be said that this periodic behaviour of the vortex axis observed for the present unstaggered vortex row in a bounded shear layer is caused by the same process as was obtained for two-dimensional staggered-vortex wakes by Zabusky & Deem (1971, figures 7 and 12). It may by conjectured, therefore, that the vortex nutation is an intrinsic feature of a two-dimensional inviscid flow arising from the interaction between the most unstable mode and the mean flow.

Figure 3 shows the time evolution of the amplitude function. It grows until $\tau = 4{\cdot}875$ and then decays. At $\tau = 8{\cdot}375$ it reaches a minimum. It should be noted that the amplitude function keeps roughly its initial gentle form during the evolution. This fact enables us to make an analytical approach to this problem, because we must first resolve the difficult problem of finding the temporal evolution of the form of the eigenfunction if the eigenfunction evolves in a complex manner.

Figure 4 shows the development of the phase function defined in (2.13). Until $\tau = 4{\cdot}875$ the phase-angle profile, which is initially antisymmetric about $x = 0$, tends to be fairly flat, and at $\tau = 4{\cdot}875$ and $\tau = 8{\cdot}375$, when the amplitude attains an extremum, it becomes almost completely flat in the entire region. If we compare the profile at $\tau = 4{\cdot}0$ (in a growing phase) with that at $\tau = 6{\cdot}0$ (in a decaying phase), we find a fairly good coincidence between their shapes.

As we have seen above, it appears that the overall spatial functional forms of the amplitude and phase eigenfunctions during the course of the nonlinear evolution remain roughly the same as those in the linear stage. In this regard, readers should notice a similar correspondence between the amplitude evolution and the phase evolution in the two-dimensional wakes examined by Zabusky & Deem (1971, figures

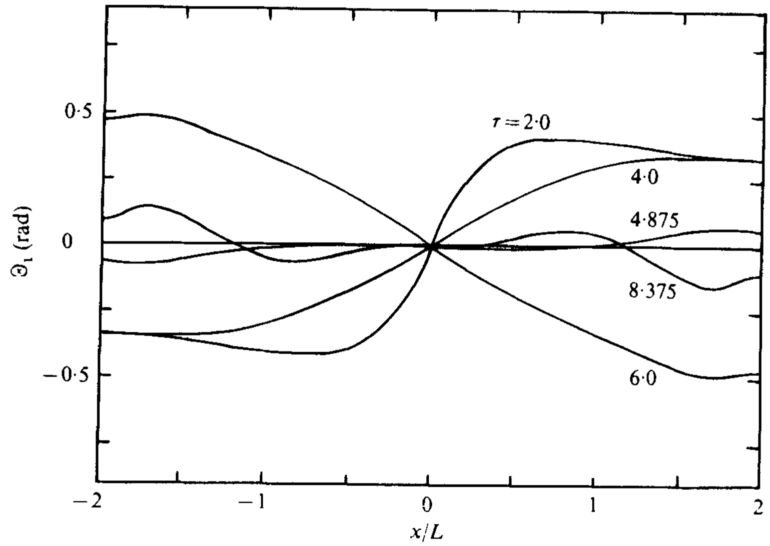

FIGURE 4. Phase functions Θ_1 of the disturbance (in radians) at several different times.

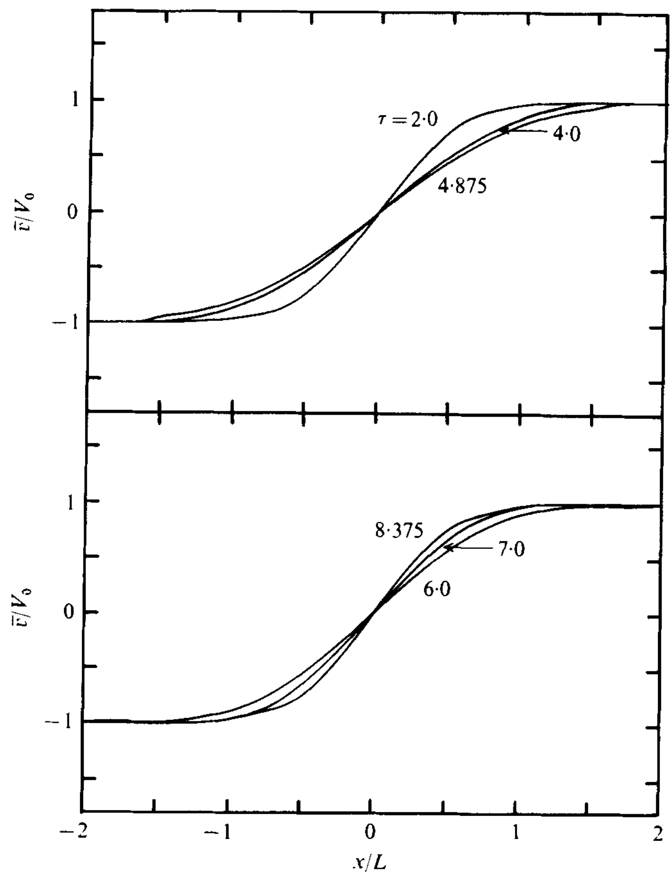

FIGURE 5. The normalized mean velocity profiles $\bar{v}$ along the x axis at different times in the growing period (top) and in the decaying period (bottom).

9, 11 and 12). Their results have clearly indicated that phase reversals occur whenever the axis of the elliptical primary vortex becomes parallel to the free-stream flow direction, the amplitude of the most unstable mode thereby reaching an extremum. An examination of their figure 9(*d*) shows that the phase profile in the growing period of the amplitude is similar to that in the decaying phase except for the sign.

Figure 5 shows how the mean velocity profile $\bar{v}$ along the x axis is modified with time. Although the overall pattern of the mean flow is not drastically changed, the gradient (or curvature) of its profile in the vicinity of the centre of the shear layer is seen to be modified considerably. Though not shown in this figure, the velocity profiles at $\tau = 2{\cdot}0$ and at $\tau = 8{\cdot}375$ are almost coincident with the initial tanh profile. This near recurrence of the initial tanh profile is observed during the subsequent evolution. From the upper half of figure 5, it is seen that the mean velocity gradient is reduced during the growing period of the amplitude, while it steepens during the decaying period (see the lower half of the figure). It may be interesting to note that such relaxation of the mean velocity gradient during the growing period was also observed for two-dimensional staggered-vortex wakes (Zabusky & Deem 1971; Sato & Kuriki 1961). Since the shear instability is very sensitive to the curvature of the mean velocity profile, it may be said that the temporal variation of the mean velocity profile is the cause of the amplitude oscillation. In the next section, we shall examine from the analytical side the relationship among the amplitude oscillation, the vortex nutation and the temporal variation of the mean flow.

In passing, we shall give the accuracy of the present calculation. As a check on the accuracy of this computation, we have monitored the total (mean flow plus disturbance) kinetic energy given in (3.10) in the next section. We have confirmed that its variation was less than 0·1 % throughout the computation.

3. Theory of vortex nutation

In this section we shall devote ourselves to deriving a nonlinear equation which describes the vortex nutation.

Substituting (2.5) into (2.1) with the aid of (2.2) and separating out the mean and disturbance parts yields

$$\frac{\partial}{\partial t}\frac{\partial^2 \phi_0}{\partial x^2} = -i \sum_{k'>0} k' \frac{\partial}{\partial x}\left(\phi_{k'}\frac{\partial^2 \phi_{-k'}}{\partial x^2} - \phi_{-k'}\frac{\partial^2 \phi_{k'}}{\partial x^2}\right), \tag{3.1}$$

$$\begin{aligned}\left(i\frac{\partial}{\partial t} - k''\bar{v}\right)\left(\frac{\partial^2 \phi_{k''}}{\partial x^2} - k''^2 \phi_{k''}\right) + k''\frac{\partial^2 \bar{v}}{\partial x^2}\phi_{k''} \\ = \sum_{k' \neq k''} k'\left[\phi_{k'}\frac{\partial^3 \phi_{k''-k'}}{\partial x^3} - (k''-k')^2\phi_{k'}\frac{\partial \phi_{k''-k'}}{\partial x}\right] \\ - \sum_{k' \neq 0}(k''-k')\left[\frac{\partial \phi_{k'}}{\partial x}\frac{\partial^2 \phi_{k''-k'}}{\partial x^2} - (k''-k')^2\phi_{k''-k'}\frac{\partial \phi_{k'}}{\partial x}\right] \quad (k'' = \pm k, \pm 2k, \ldots),\end{aligned} \tag{3.2}$$

where the summation extends over $k' = \pm k, \pm 2k, \ldots$ unless otherwise specified. Note that upon linearizing and replacing $\bar{v}(x,t)$ with $V(x)$, (3.2) reduces to the well-known

Rayleigh stability equation. Equation (3.1) can be integrated once with respect to x under the condition that $\partial\phi_0/\partial x$, $\phi_{k'} \to 0$ as $x \to \pm\infty$ to yield

$$\frac{\partial}{\partial t}\frac{\partial \phi_0}{\partial x} = -i \sum_{k'>0} k' \left(\phi_{k'}\frac{\partial^2 \phi_{-k'}}{\partial x^2} - \phi_{-k'}\frac{\partial^2 \phi_{k'}}{\partial x^2}\right). \tag{3.3}$$

It may be more convenient to express (3.3) in terms of the mean velocity $\bar{v}$, i.e.

$$\frac{\partial \bar{v}}{\partial t} = -2 \sum_{k'>0} k' \operatorname{Im}\left(\phi_{k'}\frac{\partial^2 \phi_{-k'}}{\partial x^2}\right) = -2 \sum_{k'>0} k' \frac{\partial}{\partial x} \operatorname{Im}\left(\phi_{k'}\frac{\partial \phi_{-k'}}{\partial x}\right). \tag{3.4}$$

This equation describes the distortion of the mean flow velocity through the Reynolds stress, which becomes significant in the nonlinear process. We shall now consider in more detail how the mean velocity is modified by an unstable disturbance of finite amplitude. We apply the quasi-linear analysis, which is now a classic method in the field of plasmas. If we replace $i\partial/\partial t$ with $\omega_{k''}(t)$, which is a slowly varying function of time, and neglect the mode-coupling terms in (3.2), we obtain the following quasi-linear dispersion equation:

$$(\omega_{k''} - k''\bar{v})\left(\frac{\partial^2 \phi_{k''}}{\partial x^2} - k''^2\phi_{k''}\right) = -k''\frac{\partial^2 \bar{v}}{\partial x^2}\phi_{k''}. \tag{3.5}$$

Combining this with (3.4) gives

$$\frac{\partial \bar{v}}{\partial t} = \sum_{k'>0} \frac{2k'^2\gamma_{k'}|\phi_{k'}|^2}{|\omega_{k'} - k'\bar{v}|^2}\frac{\partial^2 \bar{v}}{\partial x^2}, \tag{3.6}$$

where $\gamma_{k'}(t)$ denotes $\operatorname{Im}\omega_{k'}$. This equation takes the form of a velocity (momentum) diffusion whose effective viscosity ν_{eff} is proportional to the energy of the disturbance:

$$\nu_{\text{eff}} = \sum_{k'>0} \frac{2k'^2\gamma_{k'}|\phi_{k'}|^2}{|\omega_{k'} - k'\bar{v}|^2}. \tag{3.7}$$

What we have observed in figure 5 during the growing period of the disturbance amplitude can be explained by the velocity diffusion process described in (3.6) if we put $k' = k$.

In the above quasi-linear analysis the time evolution of the disturbance phase is not explicit. However, as we have seen in § 2, it is certain that the phase evolution of the disturbance plays the leading role in the observed vortex nutation. Therefore, in order to elucidate the fundamental process giving rise to the vortex nutation, we must take into account the time evolution of the disturbance phase. We shall next attempt to obtain an equation that can explicitly describe the phase evolution.

Since we have seen in § 2 that only the nonlinear interaction between the mean flow and the most unstable mode is responsible for the observed vortex nutation, we shall retain only the dominant mode ($k' = k$) on the right-hand side of (3.1), neglect the mode-coupling terms on the right-hand side of (3.2) and put $k'' = k$. Then by multiplying (3.2) by ϕ_k^* and adding the complex-conjugate equation, we obtain

$$\operatorname{Re}\left(\phi_{-k}\frac{\partial^2 \phi_k}{\partial x^2}\right) - k^2 \operatorname{Re}(\phi_{-k}\phi_k) - k\bar{v}\operatorname{Im}\left(\phi_{-k}\frac{\partial^2 \phi_k}{\partial x^2}\right) = 0, \tag{3.8}$$

where a dot over ϕ_k denotes differentiation with respect to t. Similarly, by subtracting the conjugate equation, we obtain

$$\operatorname{Im}\left(\phi_{-k}\frac{\partial^2\dot{\phi}_k}{\partial x^2}\right)-k^2\operatorname{Im}(\phi_{-k}\dot{\phi}_k)+k\bar{v}\operatorname{Re}\left(\phi_{-k}\frac{\partial^2\phi_k}{\partial x^2}\right)-k^3\bar{v}|\phi_k|^2=k\frac{\partial^2\bar{v}}{\partial x^2}|\phi_k|^2. \quad (3.9)$$

Equations (3.8) and (3.9), as we shall see later, describe the time evolution of the amplitude and the phase of the most unstable mode, respectively. We notice that the second derivative of the mean velocity, which has a strong influence upon the stability of a shear flow, appears on the right-hand side of (3.9), which describes the phase evolution of the most unstable mode.

Integration of (3.8) with respect to x over the entire region yields the following energy conservation equation:

$$\frac{d}{dt}\int_{-\infty}^{\infty}\left(\left|\frac{\partial\phi_k}{\partial x}\right|^2+k^2|\phi_k|^2+\frac{\bar{v}^2}{2}\right)dx=0, \quad (3.10)$$

where we have used (3.4) and the condition that ϕ_k, $\partial\phi_k/\partial x\to 0$ as $x\to\pm\infty$.

The complex amplitude $\phi_k(x,t)$ can be expressed in the form

$$\phi_k(x,t)=|\phi_k(x,t)|\exp[i\Theta_k(x,t)], \quad (3.11)$$

where

$$-\pi\leqslant\Theta_k(x,t)\leqslant\pi. \quad (3.12)$$

In the nonlinear stage, $|\phi_k|$ and Θ_k depend on both x and t, and in general it is very difficult to find a rigorous analytical solution of (3.4), (3.8) and (3.9). Fortunately, as we have seen in the previous section, the numerical analysis has guaranteed that the spatial dependence of both the amplitude and the phase function may be considered to be approximately time independent. Accordingly we shall express $|\phi_k(x,t)|$ and $\Theta_k(x,t)$ in the form

$$|\phi_k(x,t)|=A(t)f(x),\quad \Theta_k(x,t)=\theta(t)g(x), \quad (3.13)$$

where $f(x)$ and $g(x)$ are so normalized that $f_{\max}=g_{\max}=1$.

Substitution of (3.13) into (3.10) yields

$$d[A^2(1+\gamma_1\theta^2)]/dt-2\Gamma A^2\theta=0, \quad (3.14)$$

where

$$\gamma_1=\alpha^{-1}\int_{-\infty}^{\infty}f^2g'^2\,dx, \quad (3.15a)$$

$$\Gamma(t)=-\alpha^{-1}\int_{-\infty}^{\infty}k\bar{v}(f^2g')'dx, \quad (3.15b)$$

with

$$\alpha=\int_{-\infty}^{\infty}(f'^2+k^2g^2)\,dx, \quad (3.16)$$

where a prime implies differentiation with respect to x. Next, we substitute (3.13) into (3.9), multiply the result by $g(x)$ and integrate to obtain

$$\frac{d\theta}{dt}+(1+\gamma_3\theta^2)^{-1}\left(\mu+\tfrac{1}{2}\gamma_2\frac{1}{A^2}\frac{dA^2}{dt}\theta+\lambda\theta^2\right)=0, \quad (3.17)$$

where
$$\gamma_2 = -\beta^{-1}\int_{-\infty}^{\infty}(2ff'gg'+gg''f^2)\,dx, \tag{3.18a}$$

$$\gamma_3 = \beta^{-1}\int_{-\infty}^{\infty}(fgg')^2\,dx, \tag{3.18b}$$

$$\mu(t) = \beta^{-1}\int_{-\infty}^{\infty}[k\bar{v}''gf^2+k\bar{v}(k^2f^2-ff'')\,g]\,dx, \tag{3.18c}$$

$$\lambda(t) = \beta^{-1}\int_{-\infty}^{\infty}k\bar{v}f^2gg'^2\,dx, \tag{3.18d}$$

with
$$\beta = \int_{-\infty}^{\infty}[(k^2f^2-ff'')\,g^2-(2ff'gg'+gg''f^2)]\,dx. \tag{3.19}$$

As can be seen from (3.15) and (3.18), the time-dependent coefficients $\Gamma(t)$, $\lambda(t)$ and $\mu(t)$ are the functions of mean velocity $\bar{v}(x,t)$, whose time evolution is described, by substituting (3.13) into (3.4), by

$$\frac{\partial\bar{v}}{\partial t} = 2kA^2\theta\frac{d}{dx}\left(f^2\frac{dg}{dx}\right). \tag{3.20}$$

This equation indicates that the temporal variation of the mean velocity is directly proportional to θ, and hence the inclination of the vortex axis. An examination of figures 3 and 4 indicates that $(f^2g')'$ is negative for $x > 0$ and positive for $x < 0$ in the present confined free shear layer. Thus $\theta > 0$ implies relaxation of the mean velocity gradient, whereas $\theta < 0$ implies steepening. This correspondence between the evolution of the mean velocity and that of the phase inclination is consistent with what we have observed in § 2 (see figures 1 and 5).

We thus have arrived at a closed set of equations (3.14), (3.17) and (3.20) that can adequately describe the time evolution of the amplitude, phase and mean velocity.

The amplitude equation (3.14) can be rewritten as

$$\frac{dA^2}{dt} = \frac{\Gamma-\gamma_1\dot{\theta}}{1+\gamma_1\theta^2}2\theta A^2. \tag{3.21}$$

In § 2 we have shown for the confined free shear layer that, after attaining the maximum amplitude ($\theta_0 = 0$), the linearly excited most unstable (dominant) mode undergoes an oscillatory behaviour in amplitude in conjunction with the oscillation of θ_0 around $\theta_0 = 0$. As can be seen from figure 1, the phase inclination factor θ at the centre of the shear layer can reasonably be assumed to satisfy $\theta^2 \ll 1$. Since $f' \approx f/l \approx kf$ and $g' \approx g/l \approx kg$, it turns out that γ_1, γ_2 and γ_3 are all of order unity, i.e. $O(1)$. Thus we can reasonably neglect the terms $\gamma_1\theta^2$ and $\gamma_1\dot{\phi}$ in (3.21) as higher-order corrections to obtain

$$dA^2/dt = 2\Gamma\theta A^2. \tag{3.22}$$

This indicates that the growth rate of the most unstable mode is given approximately by $\Gamma\theta$ in the nonlinear stage. From (3.15*b*) we immediately find that $\Gamma(t)$ does not change its sign unless the mean velocity reverses its direction. Therefore (3.22) implies that the oscillation of θ around zero would result in an amplitude oscillation. It is further deduced from (3.20) that a periodic modulation of the mean velocity would also arise as a result of the oscillation of θ.

Since we have been able to establish that the oscillation of θ around zero (vortex nutation) is a fundamental process giving rise to the amplitude oscillation and the periodic mean velocity modulation, let us turn our attention to the phase evolution described in (3.17). Substituting (3.21) into (3.17) and expanding the second term of (3.17) in powers of θ, we obtain the following equation:

$$\dot{\theta}+\mu+(\gamma_2\Gamma-\gamma_3\mu+\lambda)\theta^2-\gamma_1\gamma_2\theta^2\dot{\theta}+O(\theta^4) = 0. \tag{3.23}$$

By differentiating μ, Γ and λ with respect to t and making use of (3.20), we obtain the following differential equations:

$$\dot{\mu} = \tilde{\omega}^2A^2\theta, \quad \dot{\Gamma} = -\epsilon\tilde{\omega}^2A^2\theta, \quad \dot{\lambda} = -\delta\tilde{\omega}^2A^2\theta, \tag{3.24a–c}$$

where
$$\tilde{\omega}^2 = 2k^2\beta^{-1}\int_{-\infty}^{\infty}[f^2g(f^2g')'''+g(k^2f^2-ff'')(f^2g')']\,dx, \tag{3.25a}$$

$$\epsilon = 2k^2\alpha^{-1}\tilde{\omega}^{-2}\int_{-\infty}^{\infty}[(f^2g')']^2\,dx, \tag{3.25b}$$

$$\delta = -2k^2\beta^{-1}\tilde{\omega}^{-2}\int_{-\infty}^{\infty}f^2g(f^2g')'g'^2\,dx. \tag{3.25c}$$

Upon differentiation of (3.23) with respect to t, it is further reduced to

$$\ddot{\theta}+\tilde{\omega}^2A^2\theta+\eta\theta\dot{\theta}-\xi\tilde{\omega}^2A^2\theta^3-\gamma_1\gamma_2\theta(\theta\ddot{\theta}+2\dot{\theta}^2)+O(\theta^4) = 0, \tag{3.26}$$

where
$$\eta(t) = 2(\gamma_2\Gamma-\gamma_3\mu+\lambda), \quad \xi = \gamma_2\epsilon+\gamma_3+\delta. \tag{3.27}$$

From (3.22) and (3.24) it is seen that the deviations of A^2, μ, Γ and λ from their values for $\theta = 0$ are of the order of θ_m (the maximum deviation of θ). Furthermore it follows from (3.25) that ϵ and δ are $O(1)$. With these considerations in mind (3.26) can be reduced to the following equation:

$$\ddot{\theta}+\tilde{\omega}^2A_m^2\theta+\epsilon[O(\theta^2)] = 0, \tag{3.28}$$

where A_m is the amplitude at $\theta = 0$ and $\epsilon[O(\theta^2)]$ contains the terms higher than θ^2. Therefore at the lowest order, the phase inclination factor θ can be expressed as a harmonic oscillation:

$$\theta(t) \simeq -\theta_m\sin(\Omega t), \tag{3.29}$$

where $\theta_m > 0$ and
$$\Omega = \tilde{\omega}A_m. \tag{3.30}$$

In (3.29) we have added a minus sign so that $t = 0$ in the above expression corresponds to $\tau = 4{\cdot}875$ in figure 1. Combining (3.22) and (3.24b) yields

$$\frac{d}{dt}\left(A^2+\frac{\Gamma^2}{\epsilon\tilde{\omega}^2}\right) = 0. \tag{3.31}$$

This may be integrated immediately to give

$$\Gamma^2 = \Gamma_0^2[1+(\epsilon\tilde{\omega}^2/\Gamma_0^2)(A_m^2-A^2)], \tag{3.32}$$

where Γ_0 is the value at $\theta = 0$. Since $\Gamma_0 = O(\gamma_{11n})$ and $\tilde{\omega} \approx 2^{\frac{1}{2}}k^2$, it is readily seen that the second term on the right-hand side of (3.32) is negligible compared with unity. It then follows that $\Gamma \approx \Gamma_0$ is a good approximation. This allows us to integrate (3.22) to give

$$A(t) = A_m\exp\{-(\Gamma_0\theta_m/\Omega)[1-\sin(\Omega t+\tfrac{1}{2}\pi)]\}. \tag{3.33}$$

We thus have obtained the phase inclination factor θ and the amplitude A as a function of time. It should be noted that the phase difference of $\frac{1}{2}\pi$ between θ and A is consistent with what we have observed in figure 1.

The period of the vortex nutation is given by

$$T = 2\pi/\tilde{\omega}A_m. \tag{3.34}$$

If we substitute $\tilde{\omega} \approx 2^{\frac{1}{2}}k^2$ into (3.34), then we obtain

$$T \approx \frac{\pi}{2^{\frac{1}{2}}}\frac{4a}{kA_m}. \tag{3.35}$$

The physical interpretation of (3.35) is as follows: kA_m represents the order of magnitude of the induced velocity of fluid particles perpendicular to the mean flow. The characteristic length $2a$ can be interpreted as a representative primary-vortex size in the direction perpendicular to the mean flow direction. Therefore (3.35) implies that the period of the vortex nutation is roughly the time required for fluid particles trapped in a vortex to travel one full circle. In other words, in the nonlinear stage, fluid particles trapped in a vortex travel around a full circle with a period of order T under the influence of the induced disturbance field of finite amplitude. Since these fluid particles transport momentum, they cause a cyclic variation in the mean velocity profile. If there is a phase difference between the mean velocity variation and the growth of the disturbance, oscillatory behaviour will appear in the amplitude evolution.

Let us now compare the period T given in (3.34) with that from the numerical calculations in § 2. In order to determine $\tilde{\omega}$ precisely, it is necessary to know $f(x)$ and $g(x)$, both of which must be calculated from the exact eigenfunctions. However, instead of seeking the exact eigenfunctions, we shall use the following simple forms:

$$f(x) = \cos(k_x x), \quad g(x) = \sin(k_x x). \tag{3.36}$$

This simplification may be justified from the numerical fact in § 2 that such a disturbance has grown with a growth rate which is almost equal to the exact linear growth rate. We make the approximation $k_x \approx k$ in (3.36), namely that the characteristic length of the eigenfunction is about equal to the longitudinal wavelength of the most unstable mode. By letting $k_x = k$ and replacing the integral limits with $\pm\pi/2k_x$ in (3.19) and (3.25), we obtain

$$\tilde{\omega} = 1{\cdot}34k^2, \quad \xi = 0{\cdot}542. \tag{3.37}$$

Substitution of (3.37) and the numerically obtained maximum amplitude A_m given by (2.16) into (3.34) gives

$$T \approx 6{\cdot}76t_0. \tag{3.38}$$

In view of the approximations we have made [neglect of higher-order terms in θ and approximation of the eigenfunctions by (3.36)], the agreement between the numerical result (2.18) ($T_0 \approx 7{\cdot}0t_0$) and (3.38) can be considered quite satisfactory.

4. Discussions and conclusions

We have shown numerically and analytically that nonlinear interaction between the most unstable mode and the mean flow leads to amplitude oscillation and vortex nutation in the nonlinear stage.

The two-dimensional, incompressible, inviscid Navier–Stokes equation is identical to the guiding-centre description of the Vlasov equation for $k_\parallel = 0$ (flute-mode assumption) and $k_\perp \rho_i \ll 1$, where $k_\parallel$ and $k_\perp$ are the wavenumbers parallel and perpendicular to the magnetic field, ρ_i being the ion Larmor radius, if ψ and ζ in (2.1) and (2.2) are read as the electric potential and the charge density, respectively (see, for example, Vahala & Montgomery 1971). This suggests that the amplitude oscillation or the quasi-periodic energy exchange between the mean flow and the most unstable mode observed by Levy & Hockney (1968) in their numerical experiment for a low density magnetized electron beam can also be explained by the present theory.

It may be interesting to note a resemblance between the amplitude oscillation for shear flow (sheared macroplasma) and that in a microplasma, like that noted between a macroplasma and a microplasma by Sato (1975). It is well known (O'Neil 1965; Al'tshul' & Karpman 1966) that resonant electrons trapped by a finite amplitude wave perform a cyclic motion in phase space. These electrons cause a cyclic variation in the resonant part of the velocity distribution function which in turn gives rise to an oscillation in the wave amplitude. If we compare the mean velocity distribution in fluids (or macroplasmas) to the velocity distribution in microplasmas, a similarity between them can be seen. In a microplasma it is said that the quasi-periodic oscillation of the wave amplitude disappears owing to phase mixing as time elapses (O'Neil 1965). Similarly, in the present case the initial phase of the disturbance will be lost and the amplitude oscillation will eventually disappear owing to phase mixing among higher harmonics which are inevitably excited by nonlinear mode couplings.

Before concluding this paper we briefly summarize the principal results that we have obtained.

(i) We have been able to show synergetically that the vortex nutation (amplitude oscillation) results from a strong nonlinear coupling between the disturbance amplitude (vorticity) and the phase. By assuming that both the amplitude function and the phase function keep the same spatial dependence as the linear eigenfunctions, we have been able to resolve the nonlinear coupled equations approximately into simple solvable equations. The solution is found to be in good agreement with the numerical solution.

(ii) Some physical interpretation of the vortex nutation is made. The oscillation period is interpreted as the period of cyclic motion of fluid particles in a vortex (see Christiansen & Zabusky 1973).

(iii) On the basis of the quasi-linear analysis it is shown that the temporal evolution of the mean flow is described by a diffusion equation. The effective viscosity is proportional to the energy of the disturbance.

The authors wish to thank Prof. T. Oguti and T. Tamao for valuable discussions and criticisms. This work was partially supported by Grants-in-Aid for Scientific Research (No. 164112) from the Ministry of Education in Japan.

Appendix

Substitution of (2.5) into (2.2*c*) yields

$$\partial^2\phi_q/\partial x^2 - q^2k^2\phi_q = -\zeta_q \quad (q = 0, \pm 1), \tag{A 1}$$

where ζ_q is the qth Fourier component of ζ. This Poisson equation is then expressed in finite-difference form as

$$\frac{1}{(\Delta x)^2}\phi_q^{j+1} - \left[\frac{2}{(\Delta x)^2} + q^2k^2\right]\phi_q^j + \frac{1}{(\Delta x)^2}\phi_q^{j-1} = -\zeta_q^j, \tag{A 2}$$

where $j = 1, 2, \ldots, J$. This gives a set of simultaneous linear equations whose coefficient matrix is tridiagonal. After separating out the real and imaginary parts, (A 2) can easily be transformed into a form amenable to numerical integration. Time integration of ζ_q is performed by simply multiplying the Fourier-expanded form of (2.1) by Δt. In the actual calculation we have used $\Delta x = 0{\cdot}04L$ and $\Delta t = 2^{-10}t_0$ (see (2.8) for L and t_0), which well satisfy the stability condition

$$\Delta x/\Delta t \gg V_0. \tag{A 3}$$

REFERENCES

AL'TSHUL', L. M. & KARPMAN, V. I. 1966 Theory of nonlinear oscillations in a collisionless plasma. *Sov. Phys., J. Exp. Theor. Phys.* **22**, 14–22.

BYERS, J. A. 1966 Confined and nonconfined interchange instabilities obtained from nonlinear computer models. *Phys. Fluids* **9**, 1038–1040.

CHRISTIANSEN, J. P. & ZABUSKY, N. J. 1973 Instability, coalescence and fission of finite-area vortex structures. *J. Fluid Mech.* **61**, 219–243.

LEVY, R. H. & HOCKNEY, R. W. 1968 Computer experiments on low-density crossed-field electron beams. *Phys. Fluids* **11**, 766–771.

MEKSYN, D. & STUART, J. T. 1951 Stability of viscous motion between parallel planes for finite disturbances. *Proc. Roy. Soc.* A **208**, 517–526.

MICHALKE, A. 1964 On the inviscid instability of the hyperbolic-tangent velocity profile. *J. Fluid Mech.* **19**, 543–556.

MICHALKE, A. 1965 Vortex formation in a free boundary layer according to stability theory. *J. Fluid Mech.* **22**, 371–383.

MOORE, R. E. & SAFFMAN, P. G. 1971 *Aircraft Wake Turbulence and its Detection.* Plenum.

O'NEIL, T. 1965 Collisionless damping of nonlinear plasma oscillations. *Phys. Fluids* **8**, 2255–2262.

SATO, H. & KURIKI, K. 1961 The mechanism of transition in the wake of a thin flat plate placed parallel to a uniform flow. *J. Fluid Mech.* **11**, 321–352.

SATO, T. 1975 Creation and annihilation of positive and negative pulses in an unstable macroplasma. *Phys. Rev. Lett.* **35**, 223–226.

SCHADE, H. 1964 Contribution to the nonlinear stability theory of inviscid shear layers. *Phys. Fluids* **7**, 623–628.

STUART, J. T. 1958 On the non-linear mechanics of hydrodynamic stability. *J. Fluid Mech.* **4**, 1–21.

TANAKA, H. 1975 Quasi-linear and non-linear interactions of finite amplitude perturbations in a stably stratified fluid with hyperbolic tangent shear. *J. Met. Soc. Japan* **53**, 1–32.

VAHALA, G. & MONTGOMERY, D. 1971 Kinetic theory of two-dimensional magnetized plasma. *J. Plasma Phys.* **6**, 425–439.

ZABUSKY, N. J. & DEEM, G. S. 1971 Dynamical evolution of two-dimensional unstable shear flows. *J. Fluid Mech.* **47**, 353–379.